UDK 67.017:669.715:539.538
Original scientific article/Izvirni znanstveni članek

ISSN 1580-2949
MTAEC9, 52(4)451(2018)

INVESTIGATION OF TRIBOLOGICAL BEHAVIOR OF AA8011-ZrB_2 IN-SITU CAST-METAL-MATRIX COMPOSITES

RAZISKAVA TRIBOLOŠKIH LASTNOSTI IN-SITU LITEGA KOMPOZITA S KOVINSKO OSNOVO AA8011-ZrB_2

Muthamizh Selvan Bellamballi Munivenkatappan, Anandakrishnan Veeramani, Duraiselvam Muthukannan

Department of Production Engineering, National Institute of Technology Tiruchirappalli-620015 Tamilnadu, India
krishna@nitt.edu

Prejem rokopisa – received: 2017-04-26; sprejem za objavo – accepted for publication: 2018-02-02

doi:10.17222/mit.2017.046

Aluminium alloy 8011 matrix composites reinforced with different weight percentages of ZrB_2 were successfully fabricated using an in-situ casting technique. X-ray diffraction and scanning electron microscopic analyses were performed to examine the presence and distribution of the reinforcements in the composites. Wear tests were performed with the weight percentage of the reinforcement, temperature, load, sliding velocity and sliding distance as the input parameters for the wear rate as response. D3 steel was used as the counterpart. The effects of various factors on the wear rate were analysed using analysis of variances. The optimal combination of the 1500-m sliding distance, 4 % of mass fractions of ZrB_2 reinforcement, 200°C temperature, 10 N load and 2 m/s sliding velocity was found to give the minimum wear rate.

Keywords: in-situ stir casting, aluminium-matrix composites, wear behavior, design of experiments

V članku avtorji opisujejo uspešno izdelavo kompozitov z matrico iz Al zlitine 8011 in ojačano z različno vsebnostjo ZrB_2. S pomočjo spektroskopije uklona rentgenskih žarkov (XRD) in vrstične elektronske mikroskopije (SEM) so določili delež in porazdelitev ojačitvene faze v izdelanih kompozitih. Izvedli so tudi teste njihove obrabe v odvisnosti od temperature, obremenitve, hitrosti in razdalje drsenja. Kot protidrsni element so uporabili orodno jeklo D3. Z analizo varianc so določili vpliv različnih faktorjev na hitrost obrabe. Ugotovili so, da je dosežena najmanjša hitrost obrabe, ko so razdalja drsenja 1500 m, masni delež ZrB_2 4 %, temperatura 200 °C, obremenitev 10 N in hitrost drsenja 2 m/s.

Ključne besede: in-situ litje s premešavanjem taline, kompoziti z matrico na osnovi Al zlitine, obstojnost proti obrabi, načrtovanje eksperimentov

1 INTRODUCTION

Metal-matrix composites (MMCs) are a type of composite material that is a macroscopic combination of two or more distinct materials with a recognizable interface between them.[1] Particle-reinforced aluminium matrix composites (AMCs) possess superior properties, such as low density, high strength-to-weight ratio, specific stiffness, good shock absorption, good dimensional stability for casting, resistance to corrosion, wear, abrasion, temperature, easy workability and easy fabrication. Due to these excellent properties AMCs are used in the applications of aerospace, automotive, electronics industries, and sports equipment. AMCs are extensively used in the fabrication of critical components like brake drums, pistons, cylinder heads, cylinder liners, drive shafts, etc. by automobile companies like Honda, Nissan, Toyota and General Motors. AA8011 alloy is used as a substitute for the AA3003 aluminium alloy to avoid problems such as contamination of the melting and holding furnaces. AA8011 is widely used in the production of semi-rigid containers and in the packaging of foods and dairy products.[2–6] Aluminium composites are fabricated with various methods such as powder metallurgy,[7] vortex method,[8] squeeze casting,[9] stir casting ex situ,[10] thermal spray deposition,[11] laser surface alloying[12] and reactive process in situ.[13] The in-situ technique has an advantage over other techniques such as the economical, uniform distribution of reinforcements, grain refinements, clear interface, good interfacial bonding strength between the matrix and reinforcement without the need of a wetting agent and a high degree of thermal stability.[14–18] From the literature, it was found that AMC's are fabricated with many reinforcements such as SiC, TiC, Al_2O_3, TiB_2, ZrB_2, in the form of oxides, carbides, nitrides, borides, fly ash, etc.[4,14,19] Among the reinforcements, ZrB_2 is a promising candidate with its excellent properties, such as high melting point (>3000 °C), high hardness, chemical inertness against molten metal, high thermal shock resistance, high wear resistance, excellent covalent bond, high corrosion resistance, better thermal and electrical conductivity, which is much needed in the aerospace applications.[14–18]

Generally, reinforced aluminium composites show superior tribological properties compared to the unreinforced aluminium alloy.[4,19] The wear behaviour of aluminium matrix composites reinforced with multi-walled carbon nano tubes was synthesized through the powder metallurgy technique. The wear resistance enhanced with the addition of multi-walled carbon nano tubes in aluminium.[20] The hybrid AA2024 with 5 % of mass fractions of SiC and graphite (0, 5 and 10) % of mass fractions fabricated by the powder metallurgy method was investigated using the pin-on-disc method to study the tribological property of the composite. The addition of the SiC and the graphite improved the wear resistance in the composite material.[21] Rao et al. fabricated the Al-Zn-Mg aluminium alloy with the SiCp (10, 15 and 25) % of mass fractions of particles using the stir-casting technique. The pin-on-disc was used for an investigation of the dry sliding wear behaviour of the materials. The wear rate of the alloy was increased due to the addition of reinforcement.[22] AA5052 was developed with ZrB_2 through the in-situ stir-casting technique. The K_2ZrF_6 and KBF_4 were the halide salts added in the molten form of aluminium, which was maintained at a working temperature of 860 °C to synthesize ZrB_2 in the AA5052 alloy. The AA5052-ZrB_2 showed improvement in the ultimate tensile strength and a 0.2 % yield strength up to 9 % of volume fractions of ZrB_2.[14] The AA6061/ZrB_2 was fabricated through the in-situ casting technique. The dry sliding wear behaviour was investigated on aluminium composites. The in-situ formed ZrB_2 particles in the aluminium alloy improved the wear resistance of the composite.[15] The in-situ composites of AA6351-ZrB_2 (0, 3, 6 and 9) % of mass fractions were synthesized by the in-situ stir-casting technique. The results indicated that the wear rate was decreased with an increase in the weight percentage of ZrB_2.[16] AA4032-TiB_2-ZrB_2 hybrid composite is fabricated through the in-situ stir casting technique. The working temperature was 850 °C. A Taguchi L25 orthogonal array is used to design the experimental trials.[17] In-situ Al composites reinforced by Al_3Zr and ZrB_2 particles fabricated with the different combinations of (10, 15, 20, and 25) %, the dry sliding wear properties of the composites were investigated. The inclusion of ZrB_2 increased the wear resistance.[23]

Design of experiments (DoE) is a statistical tool that is used in various areas such as medical, engineering, basic science, etc. to find the optimal combination of parameters, reduce the number of trials, process control and product performance prediction. The tribological behaviour of the aluminium composite reinforced with B_4C fabricated through the in-situ stir casting method was studied through designing the experimental trials with an Taguchi L27 orthogonal array. DoE was used to find the optimal combination of parameter and the influence of the parameters.[24]

From the brief literature survey it is clear that AMCs are used in real-time applications, which requires wear resistance and the addition of reinforcements in aluminium matrix, and has paved the way for the enhancement of wear resistance. The in-situ stir casting technique provides the fine and homogeneous distribution of reinforcements in the aluminium matrix in a cost-effective mode. In this paper AA 8011- ZrB_2 (0, 4 and 8) % is synthesized through the in-situ stir-casting technique and the synthesized materials are involved in X-ray diffraction (XRD), scanning electron microscope (SEM) and energy-dispersive spectroscopy (EDS) to study the presence and distribution of the ZrB_2 particles. The dry-sliding wear behaviour of the materials was investigated by conducting a pin-on-disc wear test based on the experimental plan designed through the Taguchi technique and the significance and influence of the parameters on wear behaviour of the material was identified with the help of ANOVA.

2 EXPERIMENTAL PART

2.1 Fabrication of materials

The in-situ stir-casting technique was carried out to reinforce the ZrB_2 in the AA8011 alloy, whose chemical composition is given in **Table 1**. Halide salts of K_2ZrF_6 and KBF_4 were taken to obtain the required composite proportions of weight percentage as per the literature[14,15,16,25] mixed and pre-heated at the temperature of 250 °C for 30 min to remove the moisture. The pre-weighed AA8011 matrix was melted in the graphite crucible by using electrical resistance furnace and it was maintained at 850 °C to convert it to molten form. The in-situ stir-casting process involves the addition of halide salts, i.e., K_2ZrF_6 and KBF_4, in molten form of aluminium to develop the ZrB_2 particles. The mass of salts to be added in the melt has been calculated as per the stoichiometric ratio given in **Table 2** to form composites AA8011 - 4 % of mass fractions of ZrB_2 and AA8011 - 8 % of mass fractions of ZrB_2. Stirring is done in every 5 min by using graphite rod, for maintaining the homogenous mixture of the halide salts in AA8011. The time allowed for completion of the reaction is 30 min.

The process parameters such as melting temperature, time for in-situ reaction, temperature maintained for removing moistures of halide salts and pre heating of permanent cast mould were decided through literature reviews.[14–18] The exothermic reactions that take place between molten form of aluminium and halide salts are shown in Equation (1), (2) and (3). After the completion of reaction, elements other than the ZrB_2 were evaporated or formed as slag was removed. The molten form of AA8011 was poured into the 250 °C pre-heated permanent cast iron mould and then it was formed to the desired shape and dimensions. The same procedure was followed for the fabrication of both AA8011 - 4 % of mass fractions of ZrB_2 and AA8011 - 8 % of mass fractions of ZrB_2 composites. The AA8011 without ZrB_2 is also studied to compare the wear behaviour of the AA8011 alloy and the fabricated composites.

$$3K_2ZrF_6 + 13Al \rightarrow 3Al_3Zr + 2K_3AlF_6 + 2AlF_3 \quad (1)$$

$$6KBF_4 + 9Al \rightarrow 3AlB_2 + 2K_3AlF_6 + 4AlF_3 \quad (2)$$

$$AlB_2 + Al_3Zr \rightarrow ZrB_2 + 4Al \quad (3)$$

Fabricated as-casted aluminium samples were investigated using a RINGKU XRD machine for x-ray diffraction analysis to confirm the presence of the in-situ formed ZrB_2 and AA8011 alloy. The samples were polished in different grade sheets as per the standard and etched with the Kellers etchant. Further, the presence and the distribution of the reinforcements over the matrix was explored with the scanning electron microscopic analysis along with the elemental analysis on the composites using a HITACHI SU 3000 SEM machine.

Table 1: Chemical composition of AA8011 alloy in percentage

Si	Fe	Cu	Mn	Mg	Cr	Zn	Ti	Al
0.6	0.7	0.25	0.15	0.9	0.2	0.25	0.15	Remaining

Table 2: Quantity of halide salts added for obtaining various compositions of materials.

Material Composition	Quantity of powder added (g)	
	K_2ZrF_6	KBF_4
AA8011	0	0
AA8011 - 4 *w*/% ZrB_2	100.45	200.90
AA8011 - 8 *w*/% ZrB_2	89.25	171.50

2.2 Wear testing

The tribological behaviours of materials were studied by conducting a dry-sliding wear test through the pin-on-disc method was carried out in DUCOM wear testing machine strictly followed by ASTM: G99 standards. Based on the literature[4,20,21,24] the selected parameters are: Sliding distance (m), Reinforcement (%), Temperature (°C), Load (N) and Sliding velocity (m/s). A Taguchi orthogonal array was used to optimize the number of experiments to be conducted. L18 was selected as the orthogonal array. The sliding distance was varied in two levels and the other four parameters are varied in 3 levels as shown in **Table 3**. The as-casted materials were machined to 8 mm diameter and 31 mm length. Based on earlier literature D3 steel with hardness of 63 HRC was selected as the counterpart.[4] To make the perfect contact between the pin and the counterpart, the face of the pins are polished to maintain the surface roughness of 1µm. For each experiment the samples are cleaned with acetone and weighed in the electronic weighing balance to an accuracy of 0.0001 g. To improve the accuracy of the readings, each trial was carried out 3 times and the average was taken. The wear rates for the samples were calculated through the formula given in equation (4) and the values are tabulated in **Table 3**.

$$\text{Wear rate}\left(\frac{\text{mm}^3}{\text{m}}\right)=\left(\frac{\text{Mass loss Density}}{\text{Sliding distance}}\right) \quad (4)$$

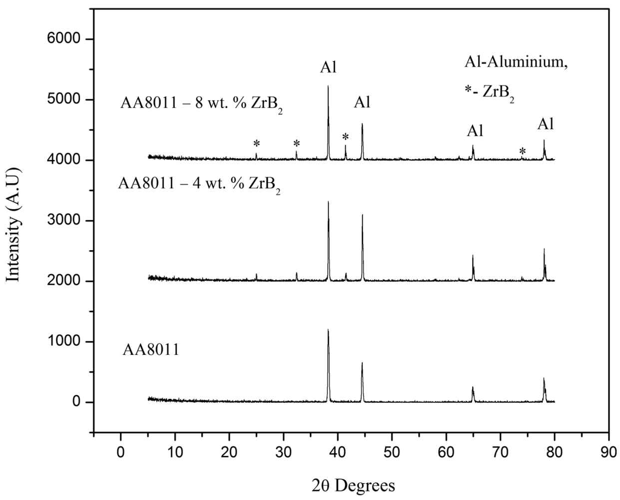

Figure 1: X-Ray diffraction results of the as-cast AA8011 and composites

Table 3: Experimental results for the wear rate

Expt. No.	Sliding distance (m)	Reinforcement (*w*/%)	Temperature (°C)	Load (N)	Sliding velocity (m/s)	Wear rate (mm^3/m)	S/N ratio
1	1000	0	35	10	1	0.003620	48.8258
2	1000	0	100	20	1.5	0.003282	49.6772
3	1000	0	200	30	2	0.003925	48.1232
4	1000	4	35	10	1.5	0.002843	50.9245
5	1000	4	100	20	2	0.003105	50.1588
6	1000	4	200	30	1	0.005046	45.9411
7	1000	8	35	20	1	0.006620	45.0053
8	1000	8	100	30	1.5	0.007976	43.1279
9	1000	8	200	10	2	0.003171	49.9761
10	1500	0	35	30	2	0.003090	50.2008
11	1500	0	100	10	1	0.002165	53.2908
12	1500	0	200	20	1.5	0.002571	51.798
13	1500	4	35	20	2	0.002264	52.9025
14	1500	4	100	30	1	0.003084	50.2177
15	1500	4	200	10	1.5	0.002070	53.6806
16	1500	8	35	30	1.5	0.004666	46.6211
17	1500	8	100	10	2	0.002711	51.3374
18	1500	8	200	20	1	0.004330	47.2702

3. RESULTS AND DISCUSSION

3.1 X-ray diffraction (XRD) analysis

The fabricated materials are exposed to X-Ray diffraction analysis to ensure the presence of ZrB_2. **Figure 1** clearly indicates the peaks equivalent to ZrB_2, which confirms the presence of ZrB_2 in the AA8011 - 4 % of mass fractions of ZrB_2 and AA8011 - 8 % of mass fractions of ZrB_2. No other significant peaks were observed in the analysis.

3.2 Micro-structural analysis

Based on the SEM images obtained as shown in **Figures 2b** and **2c**, it is evident that synthesized aluminium composites do not show any sign of common

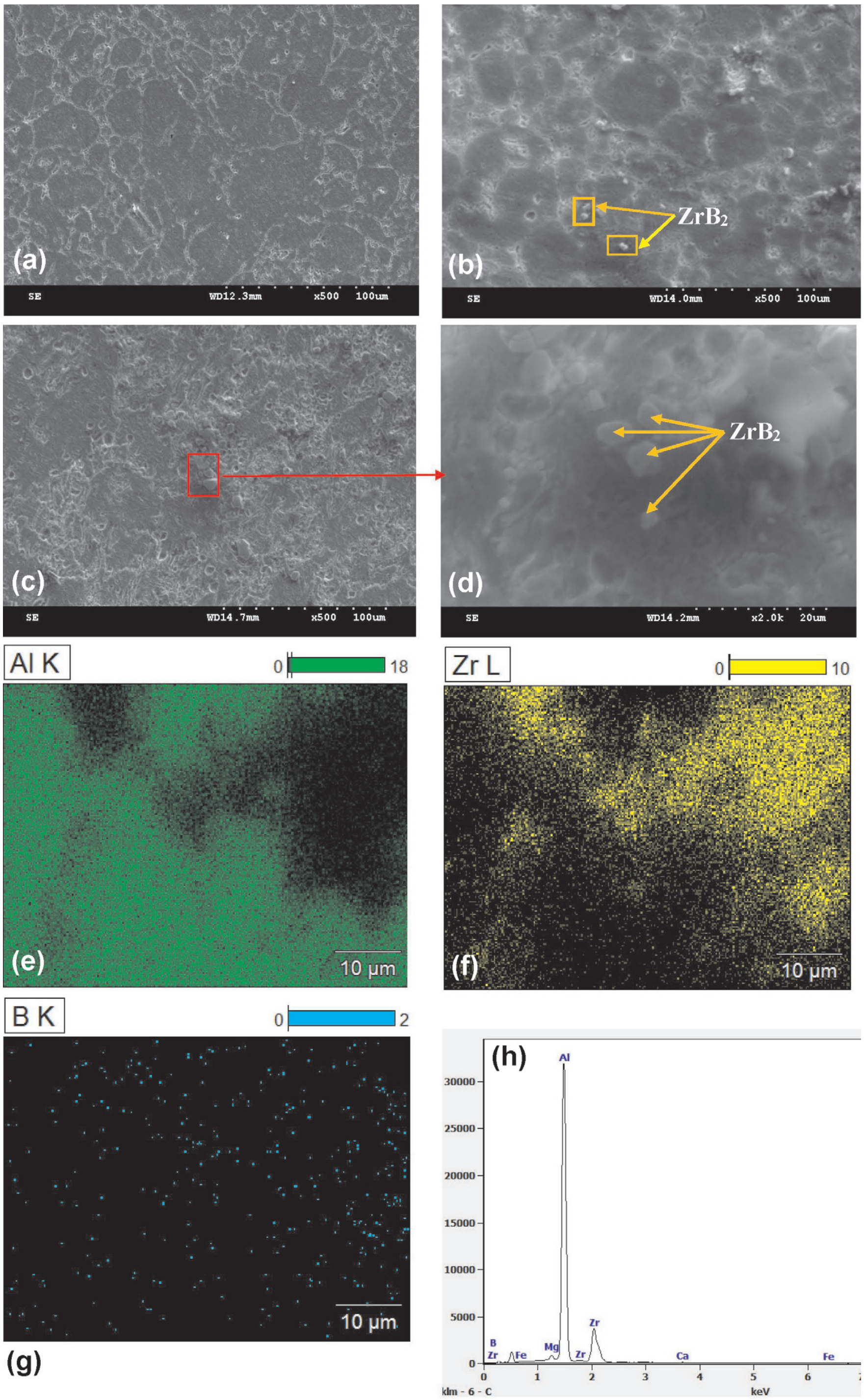

Figure 2: SEM images of: a) AA8011, b) AA8011 - 4 % of mass fractions of ZrB_2, c) AA8011 - 8 % of mass fractions of ZrB_2, d) magnified SEM image of ZrB_2. Elemental mapping of magnified ZrB_2, e) aluminium, f) zirconium, g) boride, h) EDS spectrum of **Figure 2d**

casting defects that include porosity, shrinkages, slag inclusions, etc. The density of the ZrB_2 particles in **Figure 2c** is more than **Figure 2b**, which infers that the presence of ZrB_2 in the AA8011 - 4 % of mass fractions of ZrB_2 is more than the AA8011 - 8 % of mass fractions of ZrB_2. The energy-dispersive spectroscopy and the elemental mapping shown in **Figures 2h, 2e, 2f** and **2g** confirms the presence of ZrB_2 in the aluminium matrix and the corresponding elemental analysis is given in **Table 4**. ZrB_2 distribution along the matrix is found to be homogeneous and even along the grain boundaries and the interface bond between the matrix and reinforcement has a higher strength, which tends to improve the mechanical and tribological properties of aluminium metal matrix composites. The density difference between the aluminium matrix and ceramics particles directs the properties of solidification and the homogeneous distribution of ceramic particles in an aluminium matrix. If the density of the ceramic particles is greater by 2 g/cm^3 than the matrix material, then the ceramic particle will suspend in the molten aluminium for long time, and this leads to the homogeneous distribution of ceramic particles in an aluminium matrix. In this study, the difference between the ZrB_2 particle and AA8011 matrix is observed to be greater than 2 g/cm^3. Due to the wetting action between the molten aluminium and ZrB_2 particles, the free movement of ZrB_2 gets retarded and makes the ceramic particle suspend for a greater time in the molten aluminium.[25] As mentioned in the earlier literature surveys, this work depicts the fabrication of composites through the in-situ stir-casting technique. The fabricated composites exhibit a homogeneous distribution of reinforcements in the matrix and provide a clear interfacial bond between the matrix and reinforcements.[4,14,15,17]

Table 4: Elemental analysis of energy-dispersive spectroscopy

Element	Weight (%)	Atomic (%)
Al K	73.85	90.09
Zr L	25.67	9.26
Mg K	0.48	0.64
Total	100.00	100.00

3.3 Statistical analysis

In this work the Taguchi method was used to convert the objective function to the signal-to-noise (S/N) ratio, which is a quality characteristic. The wear rate is the objective function and "lower the better" quality characteristics was selected to minimize the objective function.

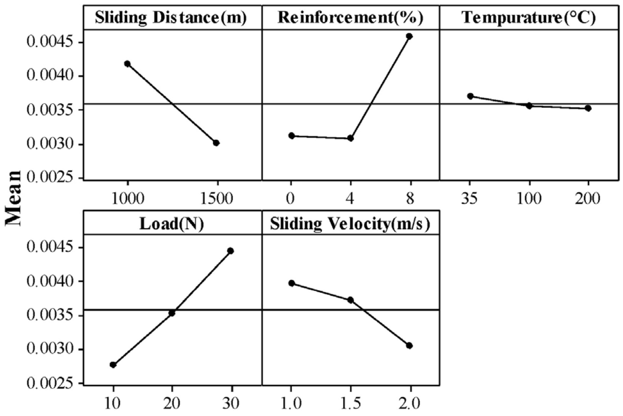

Figure 3: Main-effect plot for the wear rate

3.3.1 Analysis of factors

MINITAB-16 is used to calculate the signal-to-noise (S/N) ratio values for all the wear rates of the experiment trials in **Table 3** to analyse and to find which factors are influencing the wear rate. The most influencing factors are determined by the corresponding delta values of the factors calculated through the *S/N* ratios. The most influencing factors for wear rate are load, followed by the reinforcement, sliding distance, sliding velocity and temperature, given in the **Table 5**. The influence of the temperature is negligible. The optimal condition to obtain the minimum wear rate is a higher level of sliding distance (1500 m), middle level of reinforcement (4 %), high level of temperature (200 °C), lower level of load (10 N) and higher level of sliding velocity (2 m/s) observed from the main effect plot **Figure 3**.

The optimal combination of parameters obtained from the main effect plot is not found in the L18 orthogonal array design, so separately the experiment was carried out and the wear track is examined through the SEM. From **Figure 4a**, the wear track of the optimal combination of parameter has the smooth track which does not contain many cracks, debris, delamination and deeper grooves. The worst wear rate is observed for the AA8011 - 8 % ZrB_2 from the readings of **Table 3**, with the experimental parameters of load 30 N, sliding velocity 1.5 m/s, temperature 100 °C and sliding distance 1000 m and it was observed by the SEM, which shows many cracks, debris, micro ploughing, delamination and deeper grooves on its morphology, as shown in **Figure 4b**, these mechanisms causes the severe plastic deformation.[26,27] From **Figure 3**, the wear rate decreases with

Table 5: Response table for wear rate (smaller is better)

Level	Sliding distance (m)	Reinforcement (*w*/%)	Temperature (°C)	Load (N)	Sliding velocity (m/s)
1	47.97	50.32	49.08	51.34	48.43
2	50.81	50.64	49.63	49.47	49.30
3	-	47.22	49.46	47.37	50.45
Delta	2.84	3.41	0.55	3.97	2.02
Rank	3	2	5	1	4

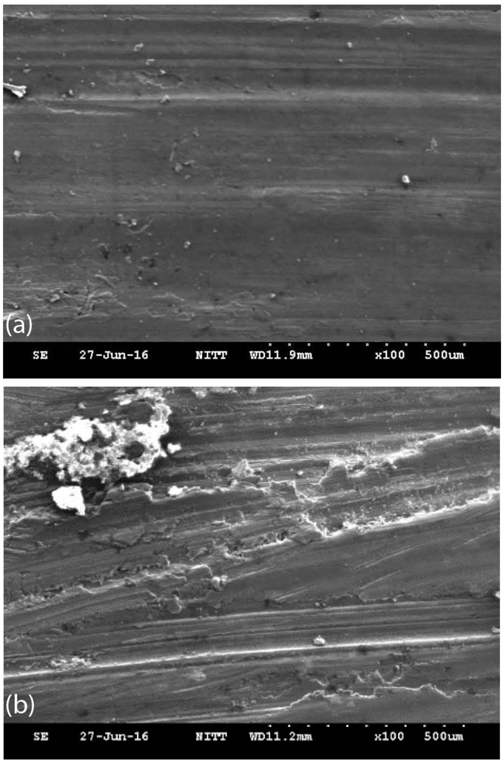

Figure 4: Wear track for: a) composite of AA8011 + 4 % mass fraction of ZrB_2 after sliding for 1500 m at a 10 N load, 2 m/s sliding velocity and 200 °C temperature b) composite of AA8011 + 8 % mass fraction of ZrB_2 after sliding for 1000 m at a 30 N load, 1.5 m/s sliding velocity and 100 °C temperature

the increase of sliding distance, at the 1000 m the wear rate is higher because the asperities which make contact with the aluminium samples are sharp and this initiates the crack. At the sliding distance of 1500 m as the distance increases, over the time asperities got compacted and blunt between the pin and the counterpart.[24] When the percentage of ZrB_2 increases the wear rate also increases, because the co-efficient of thermal expansion of ZrB_2 is more than the aluminium matrix, so this difference leads to an increase in the density of the dislocations during the solidification.[14,15] But the increase in the reinforcement is not linear with the decrease in the wear rate because the AA8011 - 4 % ZrB_2 shows better wear resistance than the AA8011 - 8 % of mass fractions of ZrB_2, which may be attributed to the occurrence of complex processes during the wear of the material.[4] When the temperature and the sliding speed increases the wear rate is decreased, as confirmed in the SEM image in **Figure 4a**, because the pin gets softer due to the formation of the thin molten layer at the asperity contacts, which is called the mechanical mixed layer (MML). It acts as a thin layer between the counterpart and pin. MML hardness is six times greater than the bulk composite.[20] When the load increases, the wear rate increases, which is indicated in **Figure 4b**.[15,23] The increase in the pressure and the contact between the pin and the counterpart leads to an increase in the frictional heat. The frictional heat between them causes the softening of the pin, which allows the asperities to easily enter into the material. This entry of asperities into the material triggers more wear rate, paves the way to mechanisms such as micro-ploughing, fracture, deformation and fragmentation.[15]

3.3.2 ANOVA analysis

ANOVA is a statistical tool used to find the most significant factors influencing the response. The analysis of the variance for the S/N ratios of the wear rate is given in the **Table 6**, which has the convincing R-sq. value of 96.48 %. The probability, given in the seventh column of Table 6, decides the influence of factors on the response. The factors which has probability less than 0.005 are the significant factors influencing the response. Sliding distance (m), reinforcement (*w*/%) and load (N) are the factors that have a more significant influence on the wear rate. Sliding velocity (m/s) and temperature (°C) failed to make any significant and influence on the wear rate. Especially temperature shows very small influence on the response.

3.3.3 Confirmation test

A confirmation experiment was conducted based on the optimal combination of parameter and obtained a wear rate of 0.000629 mm^3/m. To verify the accuracy of the experimental result, the wear rate for the optimal combination of parameter was also predicted as 0.0006033 mm^3/m with the Taguchi analysis using MINITAB-16 statistical analysis software. A minimal error of 4.25% was obtained while comparing the

Table 6: Analysis of variance for the *S/N* ratios of the wear rate

Source	Df[a]	Seq SS[b]	Adj SS[c]	Adj MS[d]	F	P[e]
Sliding distance (m)	1	36.293	36.293	36.293	57.02	0.000
Reinforcement (*w*/%)	2	42.695	42.695	21.347	33.54	0.000
Temperature (°C)	2	0.970	0.970	0.485	0.84	0.498
Load (N)	2	47.268	47.268	23.634	37.13	0.000
Sliding velocity (m/s)	2	12.368	12.368	6.184	9.72	0.007
Error	8	5.092	5.092	0.637		
Total	17	144.686				

S = 0.797822, R-Sq = 96.48 % and R-Sq (adj) = 92.52 %
[a]Degree of freedom, [b]Sequential sum of squares, [c]Adjusted sum of squares, [d]Adjusted mean squares, [e]Probability

predicted and experimental value, which validates the experimental results.

4 CONCLUSIONS

The AA8011-ZrB_2 has been successfully fabricated through an in-situ stir-casting method.

- The presence of ZrB_2 particles has been confirmed by XRD analysis.
- SEM analysis along with energy-dispersive spectroscopy analysis shows the presence of ZrB_2 and its uniform distribution over the matrix material.
- The main effect plot for wear rate, the optimal combination of parameter for obtaining minimum wear rate was identified as 1500 m sliding distance, 4 % of reinforcement, 200 °C temperature, 10 N load and 2 m/s sliding velocity.

From the ANOVA analysis the sliding distance (m), reinforcement (*w*/%) and load (N) were identified as significant factors influencing the wear rate.

- The confirmation test was carried out based on the optimal combination of parameters, the experimental wear rate was at a close range, with the predicted value having a minimal error of 4.25 %.

5 REFERENCES

[1] D. B. Miracle, S. L. Donaldson, ASM Handbook for Composites, ASM International, Materials Park, OH, USA, 2001, 1

[2] P. Jin, G. Chen, L. Han, J. Wang, Dry sliding friction and wear behaviors of $Mg_2B_2O_5$ whisker reinforced 6061Al matrix composites, Transaction of Nonferrous Metals Society of China, 24 (**2010**) 1, 49–57, doi:10.1016/S1003-6326(14)63027-2

[3] S. Prabagaran, G. Chandramohan, P. Shanmughasundaram, Influence of graphite on the hardness and wear behavior of AA6061–B_4C composite, Mater. Tehnol., 48 (**2014**) 5, 661–667

[4] S. Baskaran, V. Anandakrishnan, M. Duraiselvam, Investigations on dry sliding wear behavior of in situ casted AA7075–TiC metal matrix composites by using Taguchi technique, Materials and Design, 60 (**2014**), 184–192, doi:10.1016/j.matdes. 2014.03.074

[5] N. Ch. Kaushik, R. N. Rao, Effect of grit size on two body abrasive wear of Al 6082 hybrid composites produced by stir casting method, Tribology International, 102 (**2016**), 52–60, doi:10.1016/j.triboint. 2016.05.015

[6] K. Deliji, V. Asanovi, D. Radonji, Mechanical and corrosion properties of AA8011 sheets and foils, Mater. Tehnol., 40 (**2006**) 3, 83–85

[7] S. Mosleh-Shirazi, S. Akhlaghi, D.Y.Li, Effect of graphite content on the wear behavior of Al/2SiC/Gr hybrid nano-composites respectively in the ambient environment and an acidic solution, Tribology International, 103 (**2016**), 620–628, doi:10.1016/j.triboint. 2016.08.016

[8] M.Uzkut, Abrasive wear behaviour of SiCp-reinforced 2011 Al-alloy composites, Mater. Tehnol., 47 (**2013**) 5, 635–638

[9] W. Zhang, D. Ding, P. Gao, High volume fraction Si particle-reinforced aluminum matrix composites fabricated by a filtration squeeze casting route, Materials and Design, 90 (**2016**), 834–838, doi: 10.1016/j.matdes.2015.11.033

[10] T. Thirumalai, R. Subramanian, S. Dharmalingam, N. Radika, A. Gowrishankar, Wear behaviour of B_4C reinforced hybrid aluminum-matrix composites, 49 (**2015**) 1, 9–13

[11] R. Lukauskaite, O. Cernasejus, J. Skamat, S. Asadauskas, A. Rucinskiene, R. K. Dickuviene, N. Visniakov, Increasing the wear resistance of Al-Mg components using thermal-spray coatings, Mater. Tehnol., 51 (**2017**) 4, 673–678, doi:10.17222/ mit.2016.255

[12] L. A. B. Mabhali, N. Sacks, S. Pityana, Three body abrasion of laser surface alloyed aluminium AA1200, Wear, 290–291 (**2012**), 1-9, doi:10.1016/j.wear.2012.05.034

[13] A. A. Hamid, P. K. Ghosh, S. C. Jain, S. Ray, The influence of porosity and particles content on dry sliding wear of cast in situ Al (Ti)–$Al_2O_3(TiO_2)$ composite, Wear, 265 (**2008**) 1–2, 14–26, doi:10.1016/j.wear.2007.08.018

[14] N. Kumar, R. K. Gautam, S. Mohan, In-situ development of ZrB_2 particles and their effect on microstructure and mechanical properties of AA5052 metal-matrix composites, Materials and Design, 80 (**2015**), 129–136, doi:10.1016/j.matdes.2015.05.020

[15] I. Dinaharan, N. Murugan, Dry sliding wear behavior of AA6061/ZrB_2 in-situ composite, Transactions of nonferrous metals society of China, 22 (**2012**) 4, 810–818, doi:10.1016/S1003-6326 (11)61249-1

[16] G. Naveen Kumar, R. Narayanasamy, S. Natarajan, S. K. Babu, K. Sivaprasad, S.Sivasankaran, Dry sliding wear behaviour of AA 6351-ZrB_2 in situ composite at room temperature, Materials and Design, 31 (**2010**) 3, 1526–1532, doi:10.1016/j.matdes.2009.09.017

[17] N. V. Rengasamy, M. Rajkumar, S. S. Kumaran, Mining environment applications on Al 4032–ZrB_2 and TiB_2 in-situ composites, Journal of Alloys and Compounds, 658 (**2016**), 757–773, doi:10.1016/ j.jallcom.2015.10.257

[18] G. Gautam, A. Mohan, Effect of ZrB_2 particles on the microstructure and mechanical properties of hybrid (ZrB_2 + Al_3Zr)/AA5052 in-situ composites, Journal of Alloys and Compounds, 649 (**2015**), 174–183, dx.doi.org/10.1016/j.jallcom.2015.07.096

[19] A. P. Sannino, H. J. Rack, Dry sliding wear of discontinuously reinforced aluminum composites: review and discussion, Wear, 189 (**1995**) 1–2, 1–9, doi:10.1016/0043-1648(95)06657-8

[20] T. Rajmohan, K. Palanikumar, S. Ranganathan, Evaluation of mechanical and wear properties of hybrid aluminium matrix composites, Transactions of nonferrous metals society of China, 23 (**2013**), 2509–2517, doi:10.1016/S1003-6326(13)62762-4

[21] P. Ravindran, K. Manisekar, P. Narayanasamy, N. Selvakumar, R. Narayanasamy, Application of factorial techniques to study the wear of Al hybrid composites with graphite addition, Materials and Design, 39 (**2012**), 42–54, doi:10.1016/j.matdes.2012.02.013

[22] R. N. Rao, S. Das, D. P. Mondal, G. Dixit, Dry sliding wear behaviour of cast high strength aluminium alloy (Al–Zn–Mg) and hard particle composites, Wear, 267 (**2009**) 9–10, 1688–1695, doi:10.1016/ j.triboint.2015.12.045

[23] S. Zhang, Y. Zhao, G. Chen, X. Cheng, Microstructures and dry sliding wear properties of in situ (Al_3Zr+ZrB_2)/Al composites, Journal of Materials Processing Technology, 184 (**2007**) 1–3, 201–208, doi:10.1016/j.jmatprotec.2006.11.023

[24] N. S. Prabhakar, N. Radhika, R. Raghu, Analysis of tribological behavior of aluminium/B_4C composite under dry sliding motion, Proceedia Engineering, 97 (**2014**), 994–1003, doi:10.1016/j.proeng. 2014.12.376

[25] H. B. M. Rajan, S. Ramabalan, I. Dinaharan, S. J. Vijay, Effect of TiB_2 content and temperature on sliding wear behavior of AA7075/TiB_2 in situ aluminum cast composites, Archives of Civil and Mechanical engineering, 14 (**2014**), 72–79, doi:10.1016/ j.acme.2013.05.005

[26] W. Yi-Qi, S. Jung-il, Dry sliding wear behavior of Al2O3 fiber and SiC particle reinforced aluminium based MMCs fabricated by squeeze casting method, Transactions of nonferrous metals society of China, 21 (**2011**) 7, 1441–1448, doi:10.1016/S1003-6326(11) 60879-0

[27] D. P. Mondal, S. Das, High stress abrasive wear behaviour of aluminium hard particle composites: Effect of experimental parameters, particle size and volume fraction, Tribology International, 39 (**2006**) 6, 470–478, doi:10.1016/j.triboint.2005.03.003